Solid Freeform Fabrication 2017: Proceedings of the 28th Annual International Solid Freeform Fabrication Symposium – An Additive Manufacturing Conference
Reviewed Paper

Development of a Hybrid Manufacturing process for Precision Metal Parts

Missouri University of Science and Technology

Laser Aided Manufacturing Processes Laboratory

Department of Mechanical and Aerospace Engineering

Leon Hill, Todd Sparks, and Frank Liou

1 Abstract

This paper summarizes the research and development of a hybrid manufacturing process to produce fully dense metal parts with CNC-level precision. High performance metals, such as titanium alloys, nickel superalloys, tool steels, stainless steels, etc. can benefit from this process. Coupling the additive and the subtractive processes into a multi-axis workstation, the hybrid process, can produce and repair metal parts with accuracy. The surface quality of the final product is similar to the industrial milling capability. To achieve such a system, issues of the metal deposition process and the automated process planning of the hybrid manufacturing process will be discussed.

2 Introduction and Background

In this paper, a hybrid manufacturing system using a laser metal deposition (LMD) process is integrated with subtractive CNC milling creating a hybrid manufacturing cell. Figure 1 is a high level functional decomposition of a hybrid system. The system description can be decomposed into 4 discrete phases, as described below:

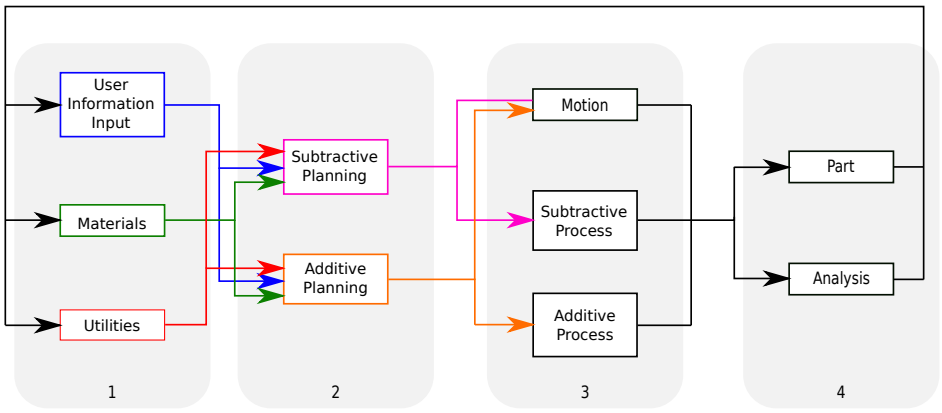

Figure 1: Functional Decomposition of Hybrid Manufacturing System

1. **Inputs** The first phase denotes the inputs into the process.

   User Information Input User information is what describes part geometry, a CAD model, and knowledge taken from pervious experience. These are the independent variables that the user has most control over.

   Materials The materials selected for the process will determine certain parameters. The user can select substrate and powder material. If the user is performing a repair, then the orignial part's material becomes a constraint.

   Utilities Hybrid systems require inputs that do not directly contribute to the output part, such as electricity, shielding gas, or machining coolant.

2. **Process planning** The second phase denotes the additive and subtractive planning is performed by CAM software and simulation software. The plan must include any premachined areas, typically necessary with part repair, and post machining after deposition [1].

   Subtractive Planning The subtractive planning step is conventional CNC machine planning.

   Additive Planning For additive planning, infill patterns, laser approach directions, powder feed rate, and part geometry will define the path plan.

3. **Manufacturing** Phase 3 is the manufacturing processes. Additive processes typicaly have poor surface finish. It is key for a hybrid manfuacturing system (HMS) to ensure the two processes do not interfere. The ability to integrate the additive and subtractive portions across all processes is key to a successful rapid high precision hybrid system [2].

   Motion There can be various tactics for moving the workpiece and/or the tool. Typical motion systems used include both CNC machines and robot arms.

   Subtractive Process The subtractive process is typically considered to be milling, but other processes, such as grinding, are a distinct possibility. Machining may be performed before and after the deposition process and is traditional CNC G-code [3].

Additive Process For the purposes of this discussion, blown powder laser deposition of metals is discussed. However, many other additive processes can be viable candidates for the hybrid treatment. When integratign with an existing motion system such as a CNC milling machine, custom M-codes must be added to denote when to turn the laser on and off, the power density, and powder delievery [3].

4. Outputs The finial phase is the output products of the hybrid system.

Part This is the desired output of the manufacturing activity.

Analysis If the part is unsatisfactory, the user inputs must be modified. Even if the part is within desired tolerances, information from the part production or repair process can be a useful feedback.

3 Tool Path Planning

3D printed parts, metal or plastic, are printed by first laying down an outline of each layer, then filling in the layer. The object must be sliced by software prior to a fill pattern path plan. Building overhangs and other complex geometries sometimes require building additional support structures. Support structures would have to be machined away later adding time and cost to the process. Using multiaxis machine capabilities, the build plan can rotate so the deposition direction is always vertical. Figure 2 illustrates how multi-axis geometry can be utilized to avoid creating support structures [3].

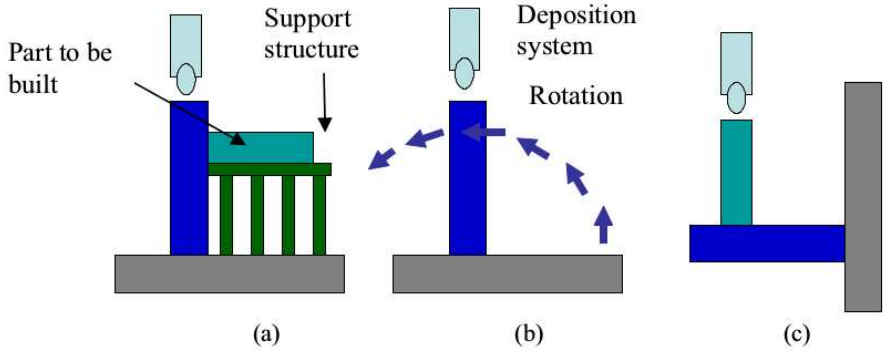

Figure 2: (a) Build part with support structure; (b) Rotation for for next portion of build (c) Post rotation, build component in different direction [3]

Path planning must also take into account uniform layer thickness and post machining path. Some circumstances may require intermediate machining processes if geometry will not allow for machining after a certain point in the LMD process. By integrating the subtractive and additive processes, machinning steps can be performed trivially saving time, money and material costs.

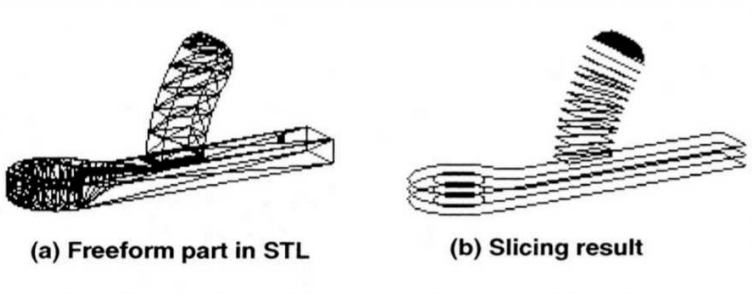

Figure 3: Multi-Axis Adaptive Slicing [4]

Figure 3 shows slices that do not have a uniform thickness. As the part must curve as it proceeds, one side of the layer must be thicker than another. Since non-uniform layers are very difficult to control in additive, a uniform section comprised of several layer is deposited. Then an intermediate machining process cuts the uniform section into a non uniform section creating the desired contour. This methodology also aids in prevent tooling crash during machining [4].

Coverage toolpath planning is very critical to depositing fully-dense metallic parts. The techniques applied to each layer effect the final product. A poorly chosen fill pattern will result in voids or over building in the final part. In order to account for variations in part geometries, an adaptive fill pattern is best suited to this task.

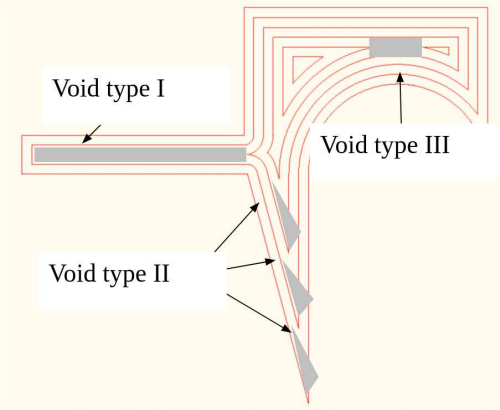

Figure 4: Different types of commonly seen voids in deposition [5]

Part geometry and poor tool path planning will lead to voids. Figure 4 illustrates common voids that occur within a part. Void type I occurs when the area to be filled is too large for a single pass, but not large enough for another parallel offset path. Void type II occurs when corner geometry has too sharp of an angle. The angle is considered too sharp depending on specific process parameters such as laser spot size. Void type III will occur if the offsetting algorithm generates more than one loop allowing a void between the separated loops.

Proper pattern planning can prevent voids from being deposited into the part. Figures 5 and 6 show the two common types of fill patterns. In figure 5 (a) is a conventional raster pattern

while (b) alternates direction each layer. Figure 6 illustrates two types of parallel offset fill patterns. The red circles denote locations where possible voids may occur. Each pattern has a geometry where it will best utilized. However, the goal of hybrid manufacturing is automating as much of the process as possible. Therefore, software must be able to determine the best pattern for a given geometry. Furthermore, the fill pattern should adapt to variations in the part geometry.

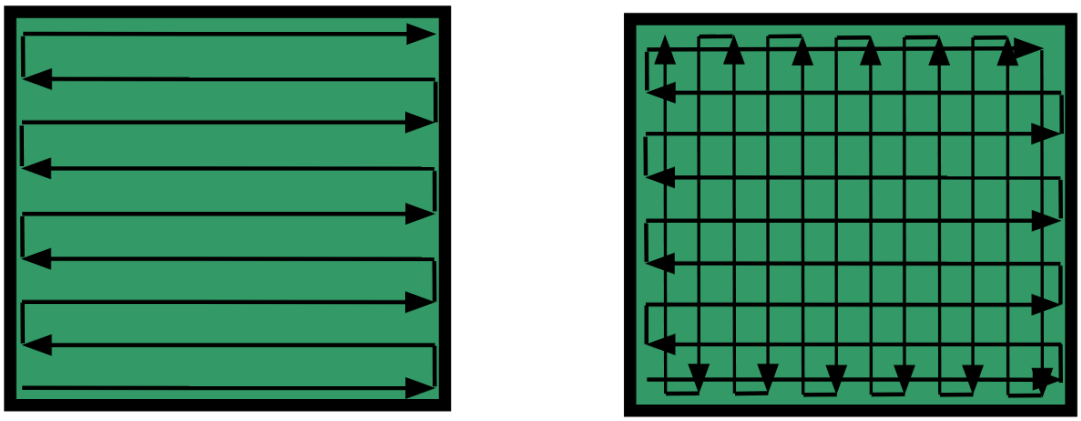

(a) Fixed direction (b) Interlaced directions

Figure 5: Different raster toolpath generation patterns [6]

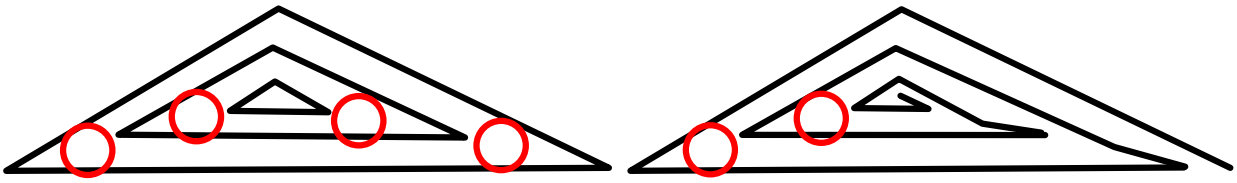

(a) Contour-parallel offset pattern (b) Spiral offset pattern

Figure 6: Deposition void occurrence for two patterns. [6]

In order to automate the planning process, possible void locations need to be addressed by software. An algorithm can be used that reliably predicts where voids will occur. The process works by comparing the area to be filled on two consecutive passes and takes the difference. The difference is compared to a user defined tolerance. If the difference is greater than the allowed tolerance, the process planning software will use a different fill pattern. Unfortunately, the tolerance required varies by material and process parameters. Thus the tolerance must be empirically determined on each machine for each material. Figure 7 illustrates the adaptive process [6].

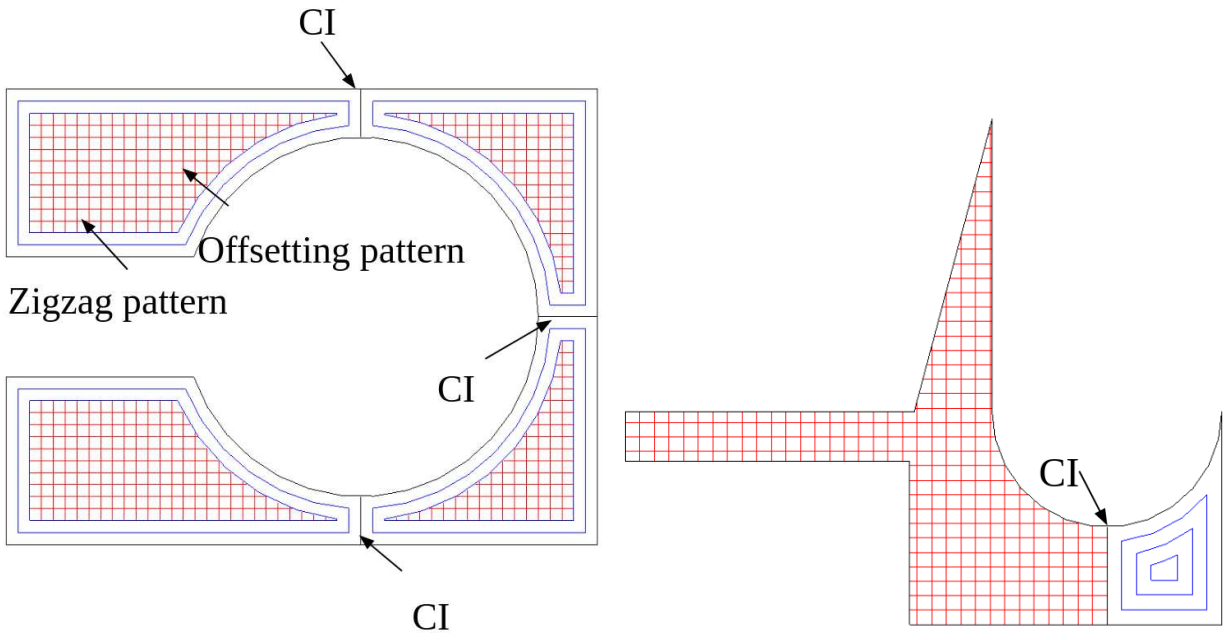

Figure 7: Adaptive toolpath for complicated geometry [6]

4 Additive Dimensional Feedback

An additive process must produce shapes as close to the CAD model as possible. The more accurate the process is, the less post machining is required allowing further savings on time and resources. This section quantifies the dimensional accuracy obtainable from LMD with closed loop height feedback control.

A part made from an additive process is built in layers. The layer thickness fluctuates throughout the part build. The layer thickness depends on the melt pool, scan speed, material mass flow rate, and laser power. The melt pool is a region where the material is molten. Variations in layer thickness are difficult to predict in simulation [7]. Layer thickness is thin compared to overall build dimensions. Therefore, most require hundreds of passes creating large error propagation.

Implementation of a sensor allows for closed loop feedback on build height. Using a pyrometer the machine can track the position of the melt pool. The measured value is compared to a reference value. The controller determines a boolean value for the melt pool position. If the melt pool is in the wrong location the machine feed rate will slow down. This allows the more material to build. Once the controller determines the melt pool to be in the proper location it will speed back up.

Planck's law, seen in wavelength form in equation 1, describes the incadsecent radiation from an blackbody at a particular wavelength and temperature. Figure 8 illustrates Planck's equation at selected wavelengths for a range oftemperatures are plotted. The pyrometer works at .45 μm and 1.8 μm. Since the laser used for deposition is 1080nm, there is no interference.

As seen in 8 the emittance drastically increases with temperature. Getting a precise temperature measurement with an optical pyrometer in an area of such high thermal gradient can be difficult, but for the purposes of this work, the sensor only needed to determine the presence or absence of the melt pool.

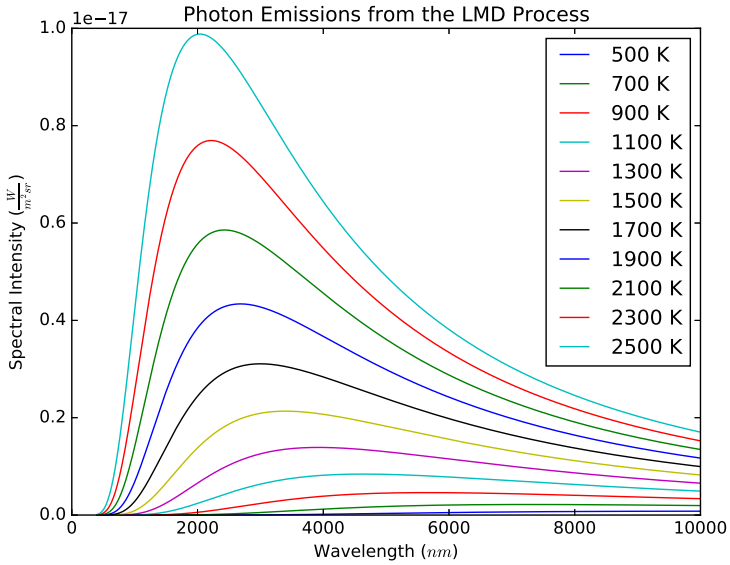

Figure 8: Spectrum radiance wavelength for temperatures

$$B_\lambda(\lambda, T) = \frac{2hc^2}{\lambda^5} \frac{1}{e^{\frac{hc}{\lambda k_B T}} - 1} \tag{1}$$

where
B_λ is the spectral radiance.
λ is the wavelength.
T is absolute temperature.
c is the speed of light.
h is Planck's constant.

The performance of a deposition system with and without a sensor can be trivially demonstrated. Figure 9 shows three parts built using the aforementioned pyrometer. Figure 10 is a part made using the same parameters as figure 9 but the layer thickness was not as simulated. Thus after several passes the melt pool was no longer on the part build surface. This demonstrates that height control can correct for improperly set parameters. The sensor does not ensure maximum efficiency, but can account for unknown materials and slight errors from simulation to practice.

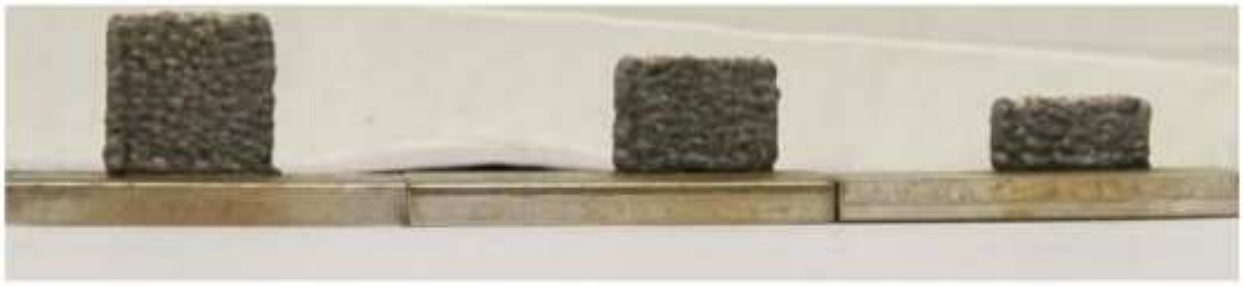

Figure 9: From left to right, sample parts made with with height feedback control at 20mm, 15mm, and 10mm [8]

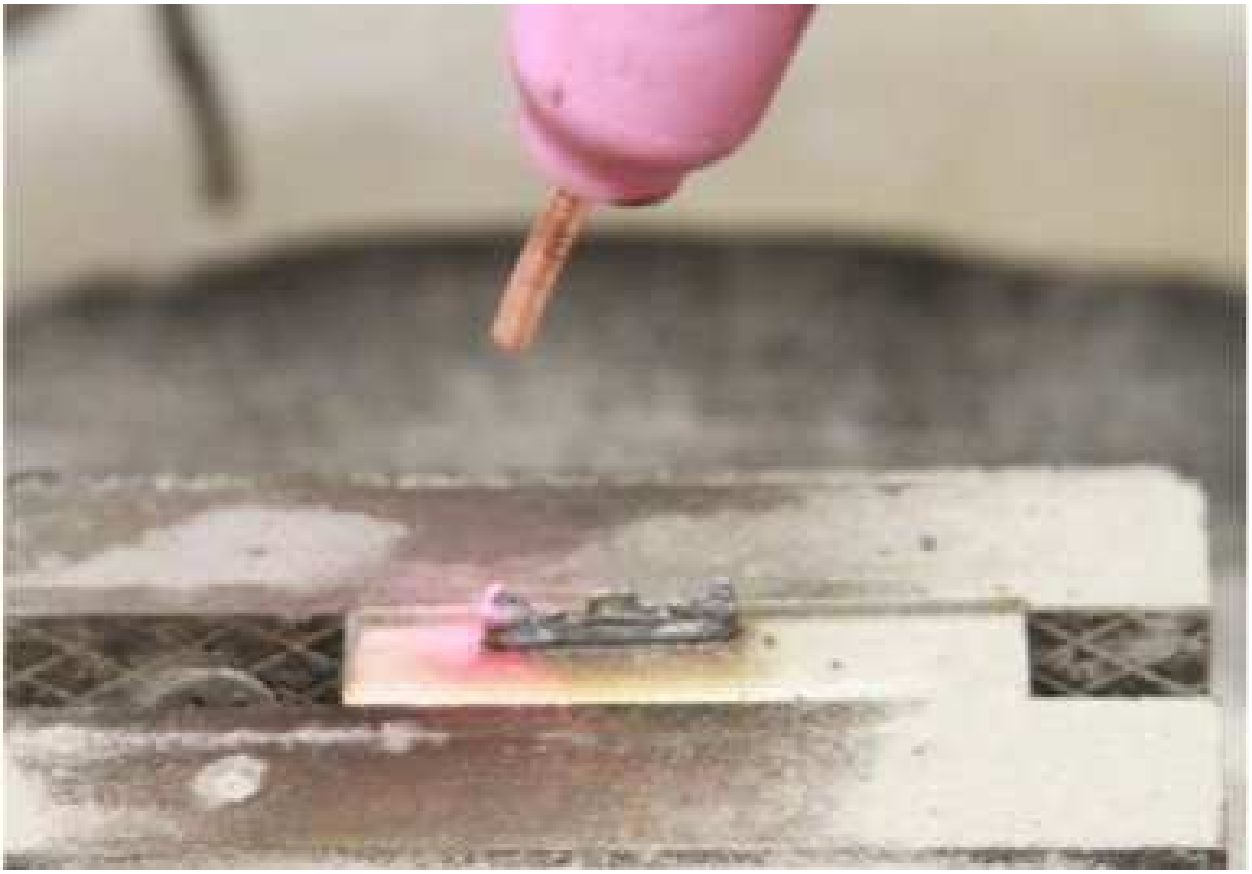

Figure 10: Parts made without height control system. The standoff distance increased quickly after a few layers. The part stopped being built up after the powder stream completely missed the melt pool. [8]

The parts built with height feedback control were built to heights of 10mm, 15mm, and 20mm. All parts had similar lengths and widths. Length differences were within 0.53 mm, and width differences were within 0.18 mm. The height differences were 0.22 mm in 10 mm parts, 0.94 mm in 15 mm parts, and 0.23 mm in 20 mm parts. The differences between the

set height and the actual height were +- 0.12mm in 10 mm parts, +- 0.49 in 15mm parts, and +- 1.02 mm in 20 mm parts [8]. In table 1 the build data is summarized.

Table 1: Accuracy and Repeatability Test Results [8]

Run #	Part Height	Measured Height	Measured Length	Measured Width	Build Time	Difference from the set height	Ra
	mm	mm	mm	mm	s	mm	μm
1	10	9.9	22.05	1.94	391.81	-0.1	93.05
2	10	9.88	21.85	1.96	392.95	-0.12	106.35
3	10	10.1	21.78	1.9	401.82	0.1	116.85
4	15	14.51	21.78	1.92	593.42	-0.049	98.9
5	15	14.92	21.25	1.96	610.03	-0.08	99.55
6	15	15.45	21.79	2.05	644.01	0.45	99.15
7	20	21.02	22.02	1.93	821.93	1.02	100.2
8	20	20.93	21.84	1.99	916.94	.93	98.85
9	20	20.79	21.72	1.87	922.44	.79	97.0

5 Machining and Verification of Deposited Part

In order to fully automate the hybrid process, hardware must be implemented to close the loop. The part dimensions must be within tolerance. Post machining is used to ensure a finished part has both the desired surface finish and dimensions. An acoustic sensor can be used to provide depth-of-cut (DOC) feedback during the post machining process. The sensor helps ensure the final part is within tolerance and provides feedback on the deposition.

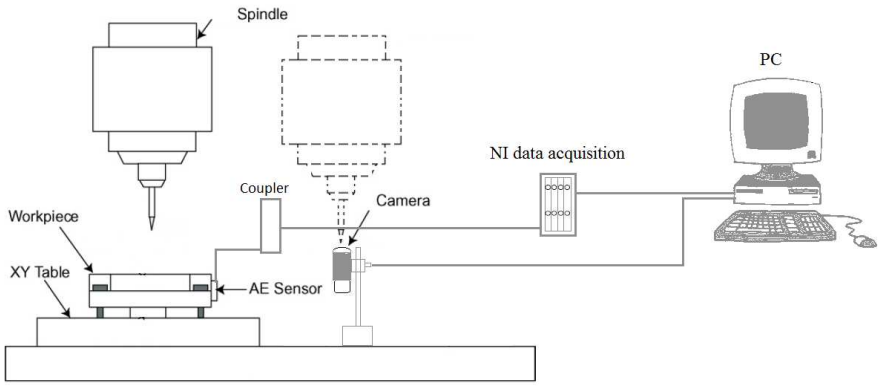

Figure 11: Experimental Components for Acoustic Emissions Sensor [9]

The acoustic sensor implements hardware and software to accurately measure the DOC during post machining. Figure 11 illustrates the sensor components. A neural network is

trained to take data from the acoustic sensor and process it. The camera is used to observe the status of the cutting tool. Its sharpness affects the acoustic emissions. This allows the neural network to adjust for variations in tool sharpness. It cannot adjust dynamically as the camera can only analyze the cutter before and after cuts.

In order to ensure accuracy of the sensor calibration cuts with known depths of cut were taken. After machining the specimen was 3D scanned and analyzed. Figures 12 and 13 show the 3D scan and the correlation between DOC and measured DOC respectively [9].

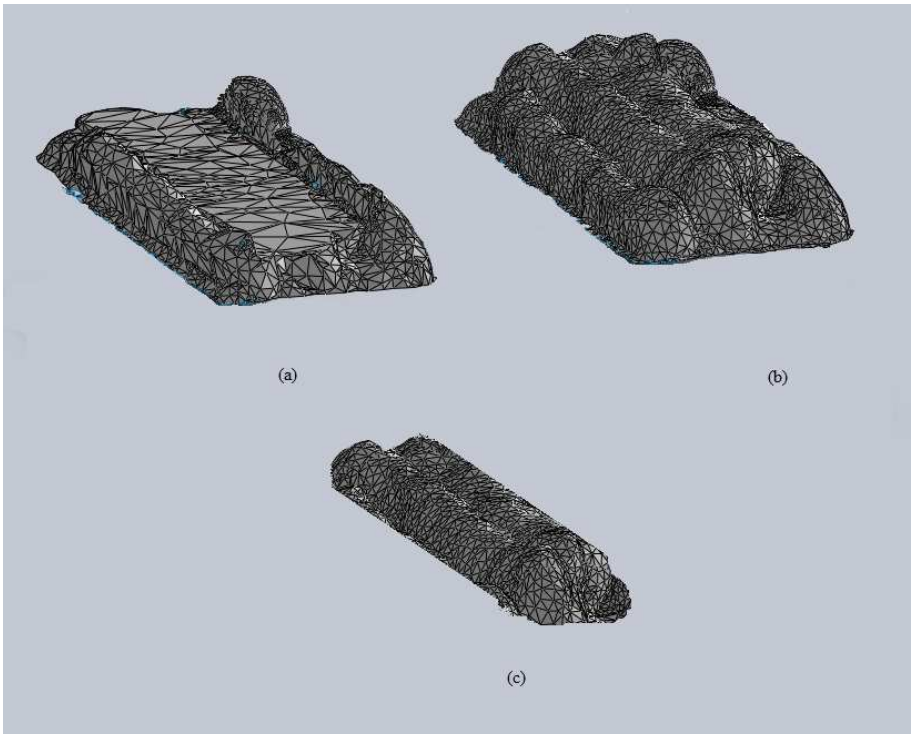

Figure 12: Scanned Deposited Material (a) Machined (b) Original (c) Removed [9]

This provides proof of concept for the acoustic emissions sensor. It allows for dynamic feedback for DOC during post machining. The sensor can be utilized to find portions of the deposit that were under or over deposited. This method can be used to provide the user with information about their deposit. Furthermore, this sensor can communicate with the controller. If a portion is under deposited, the sensor can communicate where another deposition pass should occur. Implementation of the acoustic sensor allows for more automation and less human interaction.

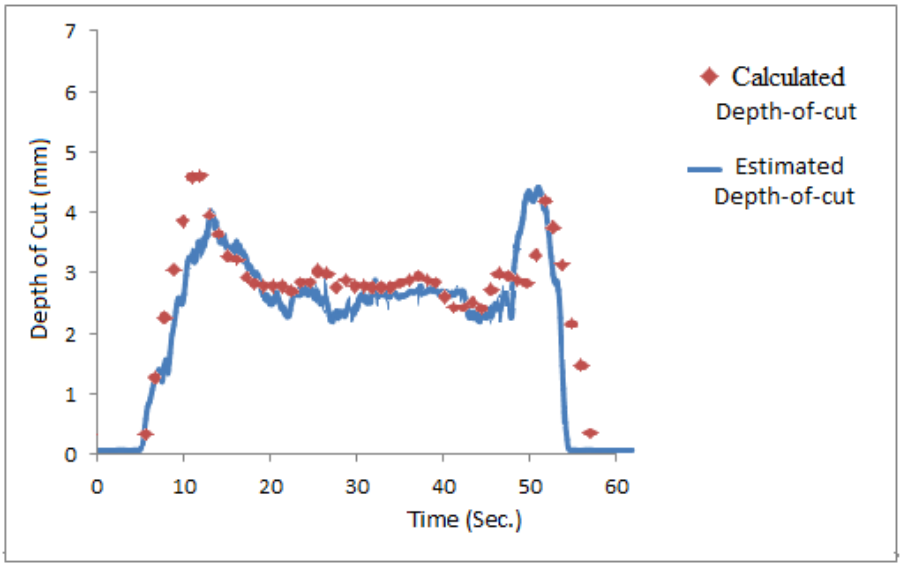

Figure 13: Measured Depth-of-cut from the Sections and Detected Depth-of-cut for a Deposited Material Detected by the Acoustic Emission Sensor [9]

6 Part Repair Using Hybrid Manufacturing

Part repair technology is a large area of focus in both military and industrial applications. As shown in figure 14 there are four main categories of damage: pitted, cracked, worn out surface, and broken.

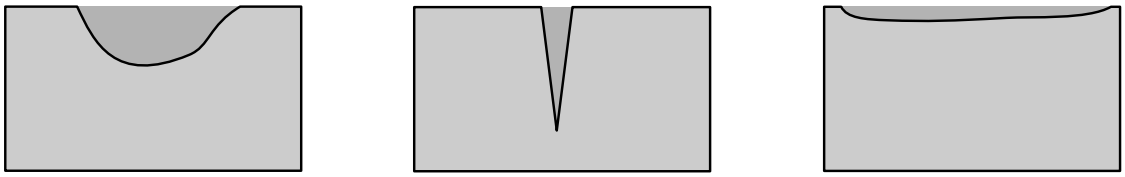

(a) Pitting (b) Cracking (c) Wear

Figure 14: Damages types [10]

Sizes of the damage is used to classify the type of damage. Pitted is considered large length and width compared to depth. Cracked is considered very small width but relatively long length. Worn out surfaces are very shallow and occur at points of contact between moving or vibrating parts.

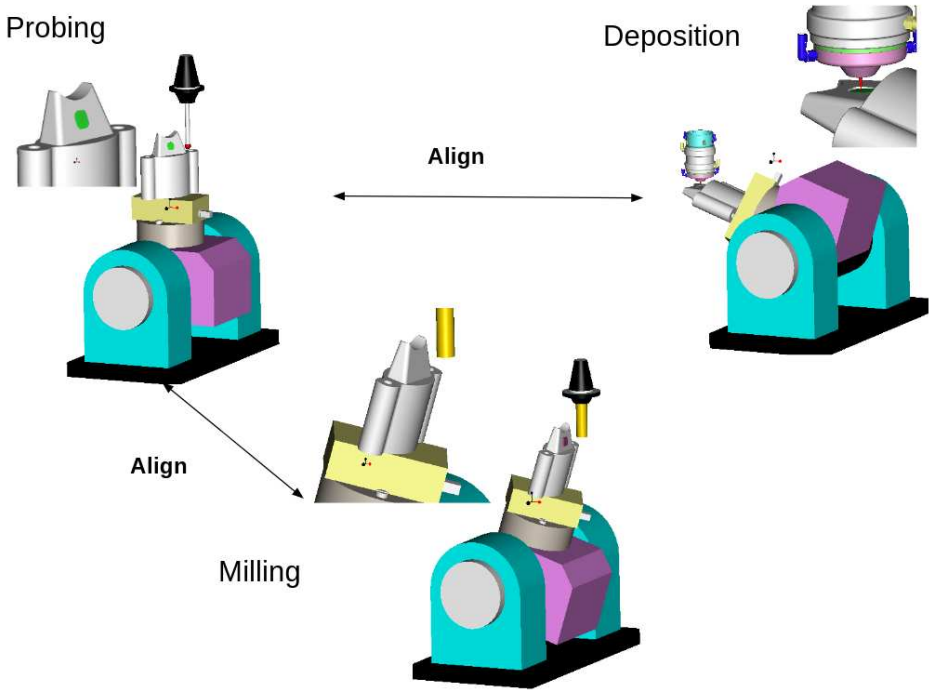

Figure 15: Repair Process [11]

Repairing a part will entail machining away the damaged area, depositing over the machined portion, post machining, then if necessary a specialized finish procedure such as grinding and polishing. The paths may be determined by Minkowski Sum and Subtraction [10]. The part must be carefully aligned to match CAD models. A touch probe with in house software can align the part allowing comparison and accurate repair [11]. On going research uses a 3D scanner and software to generate a Voxel model. The Voxel model is overlaid with a CAD model which is analyzed by software to determine the damaged regions.

For controlled repair experiments, samples were prepared with minimal machining and/or a deformation force of $3500N$. The defects were then repaired with LMD hybrid process. The repair process requires the defected area is clear of any foreign particles. The process for LMD had to be precisely planned using software. Heat transfer calculations were needed to determine time for deposition and preheating. Simulations also help ensure minimal heat affected zone (HAZ). The repaired regions were cut out into tensile test specimens and tensile tested. The results are summarized below.

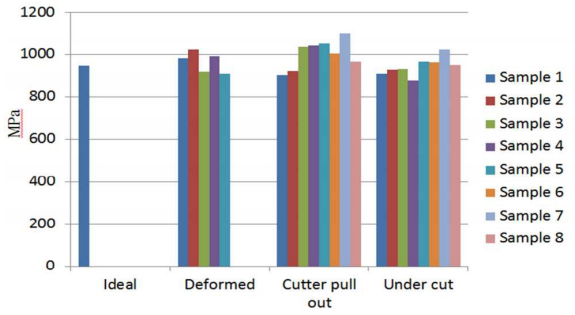

(a) Comparative Results of UTS

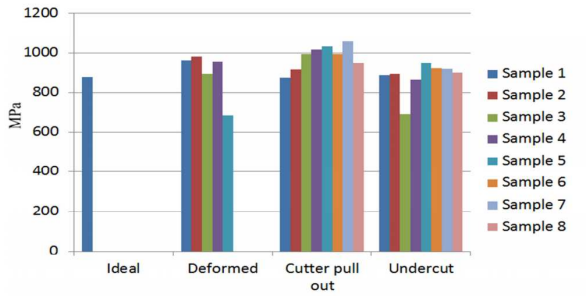

(b) Comparative Results of YS

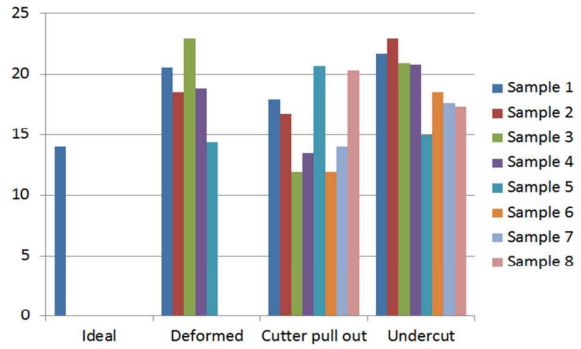

(c) Comparative Results of % Elongation

Figure 16: Mechanical testing of laser deposited Ti64 [12].

Results show the repaired Ti64 specimens conform to ideal properties of Ti64. The largest changes in properties was percent elongation. Titanium's ductility is largely dependant on the microstructure and grain size. Thus the deposited microstructure will differ from the ideal substrate microstructure. The tensile test results show a very close relationship in UTS and YS demonstrating the mechanical properties of repaired samples have not been altered to a large extent [12].

7 Mechanical Properties and Microstructure of Hybrid Manufactured Parts

High incident energy, high laser power low travel speed, result in slow cooling rates. Faster cooling rates occur when the laser power is low and the travel speed is higher. For LMD, rapid solidification with an ultra-high temperature gradient is common. With properly selected deposition parameters, an ultrafine microstructure is possible, which results in a more uniform distribution of the components. The cooling rate is directly related to the size of the substrate, layer thickness, and total number of layers deposited. New layers will melt and reform the microstructure of previous layers up to 14mm below the melt pool.

In figures 17 (a) and (b) illustrate the difference between the microstructure within the same deposit. The lower layers experience a slower cooling rate compared to the higher layers.

Therefore, the slowing cooling allows for more coarse dendrite grains to form while the faster cooling rate creates finer dendrite grains [13]

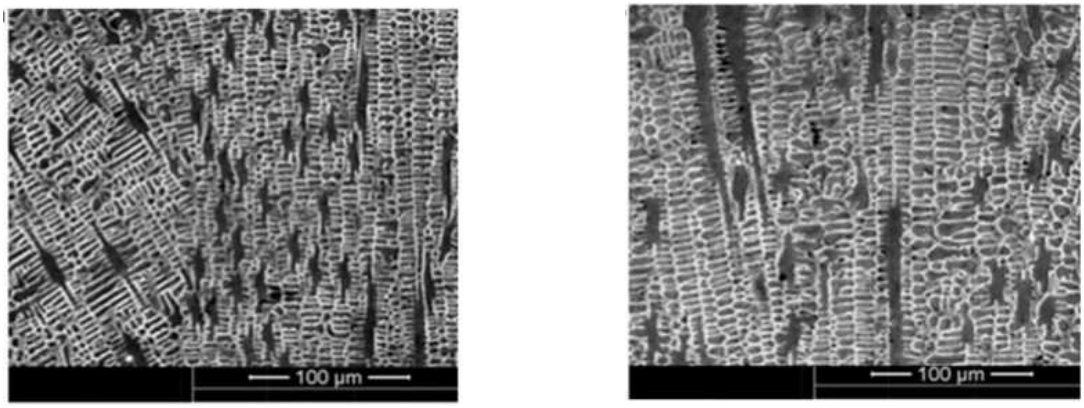

(a) Top layers (b) Bottom layers

Figure 17: 316 Stainless Steel microstructure, different positions within the laser deposition zone. [13]

Cooling rate has large impact upon the mechanical properties and microstructure. For Ti-6Al-4V, as the cooling rate decreases the α lath thickness is known to increase. The β transus plays a crucial role in determining the microstructure. The Vanadium provides the β stabilization. Cooling of the β phase determines the grain boundaries. Air cooling results in finer needle-like α phase while slow cooling forms coarse plate like α phase. Figure 18 illustrates the difference in microstructure on cooling rate.

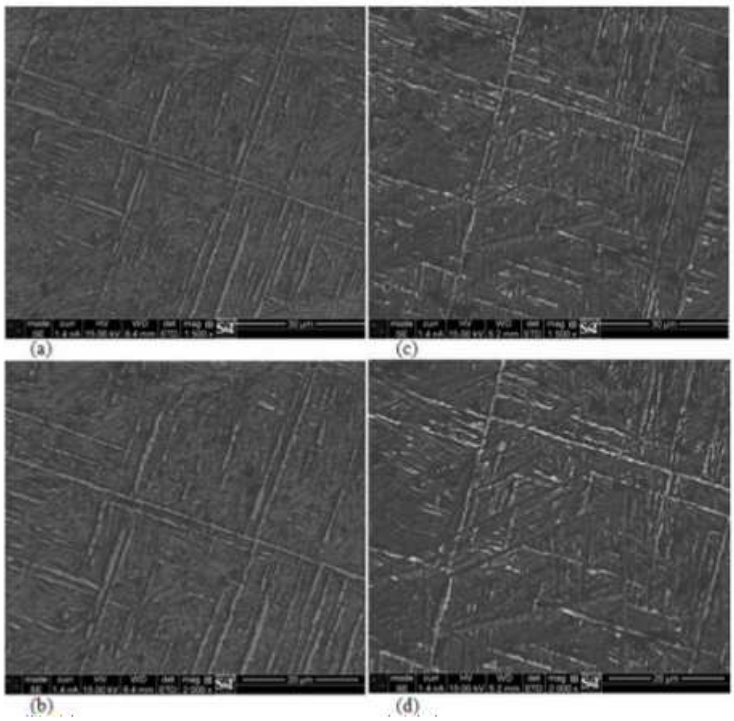

Figure 18: SEM micrographs of the Ti-6Al-4V deposit processed by laser deposition, (a,b) quicker cooling rate (c, d) slower cooling rate [14]

The mechanical properties differ depending on the properties and phase amounts present in the microstructure. With increasing the cooling rate, the width of the primary α lath decreases the aspect ratio and volume fraction of primary α increases. This increases hardness and tensile strength while decreasing the ductility. Table 2 shows the results of the tensile test according to cooling rate [14].

Table 2: Summarizing Tensile Test Data by Cooling Rate [14]

Cooling Rate	1500 C/S			5500 C/S		
	UTS (MPa)	YS (MPa)	Hardness (HV)	UTS(MPa)	YS (MPa)	Hardness (HV)
Sample 1	845	825	415	1120	995	405
Sample 2	890	835	425	1190	1140	410
Sample 3	850	830	420	1110	985	400

Typical grain size of laser deposited Ti-6Al-4V ranges between 100μm to 600μm. However, a friction stir process (FSP) can produce a forged like microstructure. The FSP modifies the base material microstructure for a highly refined α grain microstructure. A band 100μm wide did not undergo a β transformation was also observed. This 100μm band was observed around the dilution zone formed from laser interaction. The FSP refined Ti-6Al-4V is expected to increase fatigue life by delaying the fatigue crack initiation [15].

8 Conclusions

A summary of the development of a hybrid manufacturing process incorporating both laser metal deposition and CNC machining was presented. Much of the effort presented was focused on the repair application, as the hybrid process presented here has a distinct advantage over other metal additive processes when applied to repair:

- The blown powder laser deposition process is not constrained by a powder bed, so it can begin processing with arbitrary pre-existing geometry.
- The CNC machining process can produce a final surface finish not constrained by powder particle size, layer thickness, or deposited track width.

References

[1] K. Lorenz, J. Jones, D. Wimpenny, and M. Jackson, "A Review of Hybrid Manufacturing," *Solid Freeform Fabrication Symposium*, 2015.

[2] G. Manogharan, *Hybrid Manufacturing: Analysis of Integrating Additive and Subtractive Methods*. PhD thesis, North Carolina State University, 2014.

[3] F. Liou, K. Slattery, M. Kinsella, J. Newkirk, H.-N. Chou, and R. Landers, "Applications of a Hybrid Manufacturing Process for Fabrication and Repair of Metallic Structures," tech. rep., 2006.

[4] F. Liou, J. Ruan, and K. Eiamsa-ard, "Automatic Process Planning and Toolpath Generation of a Multiaxis Hybrid Manufacturing System," *Journal of Manufacturing Processes*, vol. 7, no. 1, pp. 57–68, 2005.

[5] L. Ren, F. Liou, K. Eiamsa-ard, and J. Ruan, "Part Repairing Using a Hybrid Manufacturing System," *International Manufacturing Science and Engineering Conference*, 2007.

[6] L. Ren, K. Eiamsa-ard, J. Ruan, and F. Liou, "ADAPTIVE DEPOSITION COVERAGE TOOLPATH PLANNING FOR METAL DEPOSITION PROCESS," *ASME Journal of Computing and Information Science in Engineering*, vol. International Design Engineering Technical Conference, 2007.

[7] P. Sammons, "Height Dependent Laser Metal Deposition Process Modeling," Master's thesis, Missouri University of Science and Technology, 2012.

[8] Y.-H. Pan, "Part Height Control of Laser Metal Additive Manufacturing Process," Master's thesis, Missouri University of Science and Technology, http://scholarsmine.mst.edu/masters_theses/5438?utm_source=scholarsmine.mst.edu%2Fmasters_the 2013.

[9] H. Gaja and F. Liou, "Depth of Cut Monitoring for Hybrid Manufacturing Using Acoustic Emission Sensor," *Solid Freeform Fabrication Symposium*, 2015.

[10] H. Nair, L. Ren, K. Eiamsa-ard, J. Ruan, T. Sparks, and F. Liou, "Part Repair Using a Hybrid Manufacturing System," *Solid Freeform Fabrication Symposium*, 2005.

[11] A. Padathu, T. Sparks, and F. Liou, "Workpiece Alignment for Hybrid Laser Aided Part Repair," *Solid Freeform Fabrication Symposium*, 2005.

[12] N. K. Dey, "Additive Manufacturing Laser Deposition of Ti-6Al-4V for Aerospace Repair Application," 2014.

[13] T. Amine, J. Newkirk, and F. Liou, "Microstructural and Hardness Investigation of Tool Steel D2 Processed by Laser Surface Melting and Alloying," *International Journal Advanced Manufacturing Technology*, 2014.

[14] T. Amine, J. Newkirk, and F. Liou, "Methodology for Studying Effect of Cooling Rate During Laser Deposition on Microstructure," *Journal of Materials Engineering and Performance*, 2014.

[15] R. Francis, F. Liou, and J. Newkirk, "Investigation of Forged-Like Microstructure Produced by a Hybrid Manufacturing Process," *Solid Freeform Fabrication Symposium*.